




MAGED4B Promotes Glioma Progression *via* Inactivation of the TNF- α -induced Apoptotic Pathway by Down-regulating TRIM27 Expression

Can Liu^{1,2} · Jun Liu^{2,3} · Juntang Shao^{2,3} · Cheng Huang⁴ · Xingliang Dai⁵ · Yujun Shen^{2,3} · Weishu Hou¹ · Yuxian Shen^{2,3}  · Yongqiang Yu¹

Received: 4 March 2022 / Accepted: 9 June 2022 / Published online: 20 August 2022

© Center for Excellence in Brain Science and Intelligence Technology, Chinese Academy of Sciences 2022

Abstract MAGED4B belongs to the melanoma-associated antigen family; originally found in melanoma, it is expressed in various types of cancer, and is especially enriched in glioblastoma. However, the functional role and molecular mechanisms of MAGED4B in glioma are still unclear. In this study, we found that the MAGED4B level was higher in glioma tissue than that in non-cancer tissue, and the level was positively correlated with glioma grade, tumor diameter, Ki-67 level, and patient age. The patients with higher levels had a worse prognosis than those with lower MAGED4B levels. In glioma cells, *MAGED4B* overexpression promoted proliferation, invasion, and migration, as well as decreasing apoptosis and the chemosensitivity to cisplatin and temozolomide. On the contrary, *MAGED4B* knockdown in glioma cells inhibited proliferation, invasion, and migration, as well as increasing apoptosis and the chemosensitivity to

cisplatin and temozolomide. *MAGED4B* knockdown also inhibited the growth of gliomas implanted into the rat brain. The interaction between MAGED4B and tripartite motif-containing 27 (TRIM27) in glioma cells was detected by co-immunoprecipitation assay, which showed that MAGED4B was co-localized with TRIM27. In addition, *MAGED4B* overexpression down-regulated the TRIM27 protein level, and this was blocked by carbobenzoxy-L-leucyl-L-leucyl-L-leucine (MG132), an inhibitor of the proteasome. On the contrary, *MAGED4B* knockdown up-regulated the TRIM27 level. Furthermore, *MAGED4B* overexpression increased TRIM27 ubiquitination in the presence of MG132. Accordingly, MAGED4B down-regulated the protein levels of genes downstream of ubiquitin-specific protease 7 (USP7) involved in the tumor necrosis factor- α (TNF- α)-induced apoptotic pathway. These findings indicate that MAGED4B promotes glioma growth *via* a TRIM27/USP7/receptor-interacting serine/threonine-protein kinase 1 (RIP1)-dependent TNF- α -induced apoptotic pathway, which suggests that MAGED4B is a potential target for glioma diagnosis and treatment.

Supplementary Information The online version contains supplementary material available at <https://doi.org/10.1007/s12264-022-00926-6>.

✉ Yuxian Shen
shenyx@ahmu.edu.cn

✉ Yongqiang Yu
yuyongqiang@ahmu.edu.cn

¹ Department of Radiology, The First Affiliated Hospital of Anhui Medical University, Hefei 230022, China

² Biopharmaceutical Research Institute, Anhui Medical University, Hefei 230032, China

³ School of Basic Medical Sciences, Anhui Medical University, Hefei 230032, China

⁴ Department of Pathology, The First Affiliated Hospital of Anhui Medical University, Hefei 230022, China

⁵ Department of Neurosurgery, The First Affiliated Hospital of Anhui Medical University, Hefei 230022, China

Keywords Glioma · MAGE family member D4B · Tripartite motif-containing 27 · Apoptosis

Introduction

Glioma is the most prevalent and malignant primary intracranial tumor. It reportedly represents 30% of central nervous system tumors and 80% of brain malignancies [1, 2]. Although great progress has been achieved in glioma treatment, the outcomes of patients remain poor due to its high invasiveness and recurrence rate [3, 4]. It has been shown that the median survival of glioblastoma patients is <2 years and

that the 5-year survival is <10% [5]. The discovery of cancer-specific antigens provides a powerful tool for the early diagnosis, prognosis prediction, and immunotherapy for cancer treatment. In particular, exploring the biological functions and molecular mechanisms of key genes has laid the foundation for the development of new cancer treatments.

The melanoma-associated antigen (*MAGE*) gene was first identified in the MZ-2 human melanoma cell line by Van der Bruggen *et al.* in 1991 [6]. Glial cells and melanocytes are derived from the neuroectoderm. Many reports have shown that the tumors derived from these two types of cells (glioma and melanoma) share biological characteristics in common [7]. Although *MAGE* genes have been widely studied in melanoma, these antigens are not well characterized in glioma. Based on the differences in the structure and tissue-specific expression of genes, >60 *MAGE* genes have been identified thus far and divided into types I and II [8]. Recently, *MAGE* proteins have been reported to be used as therapeutic targets in immunotherapy [9–11]. *MAGED4B* belongs to the type II *MAGE* proteins which have been reported to be strongly expressed in various types of cancer, including lung cancer [12], breast cancer [13], oral squamous cell carcinoma [14], renal cell carcinoma [15], glioma [16], and liver cancer [17]. *MAGED4B* expression has been documented to be higher in liver cancers at a more advanced pathological stage and with more tumor nodules and larger tumor sizes. Moreover, overexpression of *MAGED4B* has been found to promote tumor growth in lung cancer. These studies suggest that *MAGED4B* can be regarded as a potential cancer biomarker. However, current knowledge on the significance of the *MAGED4B* gene in glioma has been limited to tissue-level analyses and is conflicting [16, 18], and the relationship between *MAGED4B* and the occurrence and development of glioma remains obscure.

The tripartite motif-containing (TRIM) proteins, which contain RING-finger domains, constitute a large E3 ubiquitin ligase family. Currently, mounting studies have revealed that *MAGE* proteins can bind to and regulate E3 RING ubiquitin ligases. It has been reported that *MAGE*-TRIM complexes play important roles in carcinogenesis and apoptosis. In hepatocellular carcinoma, *MAGEA3* and *MAGEC2* bind to TRIM28 and promote its progression [19–21]. The tripartite motif containing 27 (TRIM27) is a member of the TRIM family [22]. Many reports indicate that TRIM27 functions to either suppress or enhance tumor development [23, 24]. In HEK293T or HepG2 cells transfected with *FLAG-TRIM27*, *FLAG-RIP1*, *FLAG-USP7*, and *Myc-Ub*, TRIM27 binds to USP7 and positively regulates TNF- α -induced apoptosis [25]. In HeLa or HEK293T cells transfected with *FLAG-TRIM27*, *FLAG-HDAC*, and *V5-NF-YC*, TRIM27 interacts with histone deacetylase (HDAC) and inhibits apoptosis [26]. It has been reported that TRIM27 binds to HDAC and inhibits apoptosis in O⁶-methylguanine-DNA

methyltransferase (MGMT)-positive glioblastoma cells [27]. However, the relationship between *MAGED4B* and TRIM ubiquitin ligases remains elusive.

In this study, we examined *MAGED4B* expression in glioma samples and analyzed the relationship between *MAGED4B* level and the prognosis. We also determined the promoting role of *MAGED4B* in the malignant biological behavior of glioma tumorigenesis and the underlying mechanisms. Our data demonstrated that *MAGED4B* is a tumor promoter in glioma by interacting with TRIM27 which induces the inactivation of the TNF- α -related apoptotic pathway.

Materials and Methods

Tissue Samples and Patient Characteristics

All paraffin-embedded clinical tissue samples (170 glioma and 30 non-cancer tissue) were collected from the Pathology Department of the First Affiliated Hospital of Anhui Medical University. No patients were treated with immunotherapy, chemotherapy, or radiotherapy before surgical resection. The present study was approved by the Hospital Ethics Committee, and informed consent was given by all patients. All specimens were confirmed and diagnosed by two pathologists according to the latest World Health Organization standards. Fresh tissues frozen in liquid nitrogen immediately after surgical resection were provided by the Department of Neurosurgery of the First Affiliated Hospital of Anhui Medical University for Western blotting and quantitative polymerase chain reaction (qPCR) analysis. This study was performed in accordance with the guidelines of the Declaration of Helsinki and approved by the Institutional Ethics Committee of the First Affiliated Hospital of Anhui Medical University (No. P2020-12-07). The animal experiment was approved by Anhui Medical University Institutional Animal Ethics Committee (No. SCXK-Wan-2017-001).

Cell Lines and Cell Culture

All glioma cell lines (U251, U138, and U87) were purchased from the Chinese Academy of Sciences (Shanghai, China). These cells were cultured in Dulbecco's modified Eagle's medium (DMEM) with 10% fetal bovine serum, and then placed in a humidified incubator (37°C, 5% CO₂).

Plasmid Vectors and Short Hairpin RNA (shRNA) Transduction

The plasmid *HA-MAGED4B* and its corresponding vector were from Guangzhou Fu Energy Gene Co., Ltd.

(Guangzhou, China). The glioma cells were transfected with DNA using Lipofectamine® 2000 Reagent (Invitrogen, Waltham, USA) according to the manufacturer's instructions. The shRNA was from Shanghai Genechem Co. (Shanghai, China). For stable knockdown of *MAGED4B*, lentiviral-transfected cells were selected with 2 mg/mL puromycin (Sigma-Aldrich, St. Louis, USA).

Immunohistochemical (IHC) Staining

Within 1 h of surgical removal, all the tissue samples were fixed in 10% neutral-buffered formalin for 20 h and paraffin-embedded using standard procedures. Serial sections were cut at 4–5 µm and mounted onto adhesion slides. The sections were stained with an anti-*MAGED4B* antibody (Sigma, St. Louis, USA) (1:500, HPA003554) at 4°C overnight, washed three times with phosphate-buffered saline (PBS), incubated with biotin for 15 min, and then washed again. Finally, 3,3'-diaminobenzidine was applied for 3 min. All sections were then re-stained with hematoxylin. As a negative control, PBS was used instead of the primary antibody [28]. The final immunoreactivity scores of the sections were obtained by multiplying the percentage score and the intensity score. As described previously [29], the positive percentage score was recorded, and the intensity score was defined as 0 (negative), 1 (weakly positive), 2 (moderately positive), or 3 (strongly positive). The final *MAGED4B* gene staining score was the product of the percentage and intensity score (ranging from 0 to 300). X-tile (Yale School of Medicine, CT, USA) was used to analyze the scores [30]. In addition, a score of 140 was used as the cut-off value. Samples with scores >140 were defined as having high expression of *MAGED4B*.

Quantitative Real-time PCR (qRT-PCR)

According to the manufacturer's instructions, TRIzol reagent (Invitrogen, Carlsbad, USA) was used to extract total RNA from tissues, and a complementary DNA (cDNA) Reverse Transcription Kit (Takara, Japan) was used to reverse transcribe total RNA into cDNA. Then, qRT-PCR assay was carried out using SYBR Green PCR Master Mix. The primer sequences used were as follows: *MAGED4B* (forward: 5'-CCAGAATCAGAACCGAGA-3'; reverse: 5'-CCAAA TCTCCGTCTCA-3'), and *GAPDH* (forward: 5'-GAAGGT GAAGGTCGGAGTC-3'; reverse: 5'-GAAGATGGTGAT GGGATTTTC-3').

Western Blot Analysis

Total cell protein was extracted with sodium dodecyl sulfate (SDS) lysis buffer (250 mmol/L Tris-HCl, pH 7.4, 2.5% SDS)

and then quantified using the bicinchoninic acid (BCA)-based Protein Assay (Thermo Fisher Scientific, Shanghai, China). The same amount of protein extract (50 µg) was loaded onto 15% SDS PAGE gels for electrophoresis, and then transferred to PVDF membranes. The membrane was blocked in 5% skim milk for 1 h at room temperature and then incubated overnight at 4°C with the following antibodies: anti-*MAGED4B* (Sigma, 1:500, HPA003554), anti-PCNA (Cell Signaling Technology, Danvers, USA) (1:1,000, 13110S), anti-E-cadherin (BD, Franklin Lakes, USA) (1:1,000, 610182), anti-β-catenin (BD, 1:1,000, 37447), anti-vimentin (Abcam, Cambridge, UK) (1:1,000, ab92547), anti-HA (Sigma, 1:1,000, H6908), anti-*TRIM27* (Proteintech, Wuhan, China) (1:2,000, 12205-1-AP), anti-caspase-3 (Cell Signaling Technology, 1:1,000, 9662), anti-cleaved-caspase-3 (Affinity Biosciences, OH, USA) (1:1,000, AF7022), anti-caspase-8 (Boster, Wuhan, China) (1:1,000, A00042), and anti-RIP1 (Boster, 1:1,000, BST21824850). The membrane and the corresponding secondary antibody were incubated for 1 h at room temperature. Finally, the blots were developed using a chemiluminescence system (Bio-Rad, Hercules, USA).

Cell Counting Kit-8 (CCK8) Assay

Following treatment with plasmid or shRNA, the cells were inoculated in 96-well plates (2,000–5,000 cells/well). After the cells were incubated for 1–3 days, 10 µL CCK8 reagent (Beyotime, China) was added to each well at a ratio of 1:10 and incubated at 37°C for 1 h. Finally, the absorbance of each well was measured with a microplate reader (Biotek, Vermont, USA) at 450 nm.

Determination of the Half-maximal Inhibitory Concentration (IC₅₀)

Cells treated with shRNA or plasmid were seeded in 96-well plates (5,000 cells/well). Three multiple parallel wells were set up in each group. The cells were treated with different concentrations of cisplatin (32, 16, 8, 4, 2, and 1 µg/mL) (Sigma) for 24 h or temozolomide (TMZ) (160, 80, 40, 20, 10, and 5 µg/mL) (MCE, Shanghai, China) for 48 h, and then the CCK8 assay was used to determine the cell viability in each well. The IC₅₀ was calculated using the regression model in SPSS 17.0 (SPSS Inc., Chicago, USA).

Colony-formation Assay

The cells were inoculated into 6-well plates at 400 cells per well and incubated at 37°C for 10–14 days. The cells

were then fixed in methanol for 20 min and stained with 0.1% crystal violet dye for 20 min. Finally, colonies with >50 cells were counted using an inverted microscope and photographed.

Cell Migration and Invasion Assays

The invasive ability of cells was measured using Transwell chambers (8- μ m pore membranes; Corning Inc., New York, USA). Beforehand, Matrigel (50 μ L; BD) was smeared at the bottom of the membrane of the chamber. Glioma cells (1×10^4) were inoculated into the upper chamber, and 500 μ L medium containing 20% fetal bovine serum was added to the lower chamber. After 24 h, the cells were fixed with methanol, and the Matrigel and cells in the upper chamber were wiped off. The cells at the bottom of the chambers were then stained with 0.1% crystal violet. Finally, five visual fields were selected for each compartment and then counted at 100 \times under a light microscope.

Wound-healing Assay

Cells were transfected, inoculated in a 6-well plate, and cultured to 70%–80% confluence. The monolayer of cells was scratched with a yellow pipette tip to generate scratch wounds, and then wound closure was photographed at 0 h and 72 h using an inverted microscope. The results were analyzed using ImageJ software (NIH, Wayne Rasband, USA).

Cell Cycle and Apoptosis Assay

Cell cycle and apoptosis were assessed by flow cytometric analysis (BD Biosciences). The cells were collected and fixed in 70% ethanol at -20°C for 24 h, and then stained with propidium iodide (PI, Sigma) for cell cycle analysis. For apoptosis analysis, the cells were treated using an Annexin V-APC/PI kit (Bestbio, Shanghai, China) according to the manufacturer's instructions. Finally, the apoptotic index was measured by flow cytometry.

5-Ethynyl-2'-deoxyuridine (EDU) Assay

The cells from different treatment groups (2,000–5,000 cells per well) were inoculated in a 96-well plate and cultured in an incubator for 24 h. The cells were analyzed using an EdU kit according to the manufacturer's instructions (RiboBio, Guangzhou, China). The stained images were observed and photographed under a fluorescence microscope, and five visual fields were randomly selected to calculate the positive EDU rate.

Terminal Deoxynucleotidyl Transferase (TdT)-mediated dUTP-biotin Nick End Labeling (TUNEL) Assay

Cells from different treatment groups (2,000–5,000 cells per well) were seeded in 96-well plates, cultured in an incubator for 24 h, and then treated with cisplatin (8 μ g/mL) for 24 h or TMZ (40 μ g/mL) for 48 h. The TUNEL kit (Ribobio, Guangzhou, China) was used to assess apoptosis according to the manufacturer's instructions. The stained images were observed and photographed under a fluorescence microscope, and five fields of view were randomly selected to calculate the results.

Tumor Orthotopic Assays in Nude Rats

All experimental protocols were approved by the Animal Ethics Committee of Anhui Medical University and were carried out in accordance with the guidelines of Anhui Medical University. Male nude rats aged 6–8 weeks were purchased from Beijing Charles River Laboratory Animal Co., Ltd (Beijing, China). After the rats were anesthetized (10% chloral hydrate, 3 mL/kg, intraperitoneal injection), they were placed prone on a stereotactic head frame, and a scalp incision was made along the sagittal suture. A hole 1 mm in diameter was drilled in the skull, located 1 mm anterior to the coronal suture and 3 mm mediolateral from the midline. PBS or U87 cells stably transfected with negative control shRNA (sh-NC) or sh-*MAGED4B* (1×10^6 in 10 μ L PBS) were injected into the brains of nude rats with a micropipette syringe at 1 μ L/min. The injection site was the left caudate/putamen at a depth of 6 mm. After the injection, the needle was slowly pulled out after 5 min, the hole was sealed with bone wax, and the wound was sutured. Sixteen days after the injection, a magnetic resonance imaging (MRI) scanner was used to assess the tumor burden of the nude rats and to measure tumor volume. Subsequently, the rats were euthanized, and their brains were extracted, fixed in 4% paraformaldehyde for 48 h, and embedded in paraffin blocks for immunohistochemical analysis.

Immunofluorescence Assay

Cells were grown on glass discs in a 24-well plate and fixed with 4% paraformaldehyde for 30 min, and 0.3% Triton solution was added to penetrate the nucleus. The cells were then incubated with the primary antibody overnight at 4°C . In the dark, a fluorescent dye-coupled secondary antibody and DAPI stain were used to detect the location of the primary antibody and the nucleus. Images of the fixed cells were acquired using a confocal laser scanning microscope.

Co-immunoprecipitation (Co-IP)

Co-IP was applied as previously reported [31]. Protein A beads mixed with the anti-TRIM27 antibody were used for analysis. Next, total cell proteins were immunoprecipitated with these agarose beads and then eluted. The indicated proteins were detected using Western blotting. We used the light chain-specific secondary antibody (1:4,000, Protein-tech, SA00001-7L) to avoid overlap of the TRIM27 band position with the heavy chain.

Statistical Analysis

SPSS 17.0 and GraphPad Prism 5.0 (San Diego, USA) software were used for statistical analysis. The differences between two groups were analyzed by Student's *t*-test, and multiple groups were analyzed by one-way analysis of variance (ANOVA) followed by Tukey's test. The χ^2 test was used to evaluate the correlation between MAGED4B expression and clinicopathological features, and the Kaplan-Meier method was used for survival analysis. Univariate and multivariate analyses were performed using Cox regression. All quantitative data are presented as the mean \pm SD. A *P*-value <0.05 was considered statistically significant.

Results

MAGED4B Is Up-regulated in Human Glioma Samples

We first analyzed the *MAGED4B* messenger RNA (mRNA) expression levels in gliomas using Oncomine (<https://www.oncomine.org/resource/login.html>) and Gene Expression Profiling Interactive Analysis (GEPIA) (<http://gepia.cancer-pku.cn/>) datasets [32]. We found that the *MAGED4B* mRNA level was significantly up-regulated in glioma compared with non-cancer tissue (Fig. S1A–C). We next assessed the *MAGED4B* mRNA levels in 8 randomly selected paired glioma tissues and adjacent non-cancer specimens *via* qPCR assay. Similarly, as shown in Fig. 1A, the *MAGED4B* mRNA level in glioma tissue was much higher than that in non-cancer tissue. These results indicate that *MAGED4B* is up-regulated in glioma at the transcriptional level. We also measured the *MAGED4B* protein levels in 8 paired primary glioma samples and the corresponding adjacent tissue by Western blotting. Accordingly, the *MAGED4B* protein level was significantly higher in glioma samples than in non-cancer tissues (Fig. 1B). As shown in Fig. 1D, *MAGED4B* expression was significantly higher in glioma than in non-cancer tissue. Therefore, our data indicate that both the mRNA and protein levels of *MAGED4B* were significantly increased in glioma. In addition, we found that the worse the tumor grade, the

higher the *MAGED4B* level in glioma samples, consistent with the results of Oncomine database analysis (Fig. S1D).

Relationship Between MAGED4B Expression and Clinical Features of Glioma

To assess the effect of *MAGED4B* on glioma progression, we analyzed the relationship between *MAGED4B* expression and the main clinicopathological characteristics of glioma patients (Table 1). *MAGED4B* expression was significantly associated with tumor grade ($P = 0.008$), patient age ($P = 0.007$), and tumor diameter ($P = 0.042$). Ki-67, a widely used marker of cancer cell proliferation, was closely associated with a poor prognosis in glioma patients. As shown in Table 1, up-regulated *MAGED4B* expression was related to Ki-67 overexpression ($P = 0.010$), which was consistent with the results of the analysis of the Tumor Immune Estimation Resource (TIMER) database (<http://timer.comp-genomics.org/>) (Fig. S2). However, *MAGED4B* expression was not significantly associated with gender ($P = 0.538$), P53 level ($P = 0.538$), or CD34 molecule level ($P = 0.094$). Furthermore, the relationship between *MAGED4B* and the prognosis of glioma was evaluated using the Cox proportional-hazards regression model (Table 2). The univariate analysis results indicated that patient age ($P < 0.001$), Ki-67 level ($P < 0.001$), P53 level ($P = 0.001$), tumor grade ($P < 0.001$), and *MAGED4B* expression ($P = 0.002$) were associated with the overall survival (OS) of glioma patients. The multivariate analysis data demonstrated that *MAGED4B* expression ($P = 0.006$) and tumor grade ($P = 0.001$) were significant predictors of OS in glioma patients. Moreover, Kaplan–Meier survival analysis showed that glioma patients with high *MAGED4B* expression and advanced tumor grade had significantly shorter survival (Fig. 1E, F). Survival analysis using the GEPIA database showed that the patients with a high *MAGED4B* level exhibited lower OS and disease-free survival than patients with a low *MAGED4B* level (Fig. 1G, H). These findings indicate that *MAGED4B* is a prognostic factor for poor survival in glioma patients.

Screening *MAGED4B* shRNA and Identifying the Knockdown Efficiency in Glioma Cell Lines

Analysis of data from the Cancer Cell Line Encyclopedia (<https://portals.broadinstitute.org/ccle>) and The Human Protein Atlas (<https://www.proteinatlas.org/>) datasets indicated that *MAGED4B* mRNA was significantly elevated in glioma cell lines, especially in U87 cells (Fig. S3). To verify the analysis, we assessed the *MAGED4B* level in three glioma cell lines using Western blot analysis. Consistently, the *MAGED4B* protein level was the highest in the U87 cell line and lower in the U251 cell line (Fig. 2A).

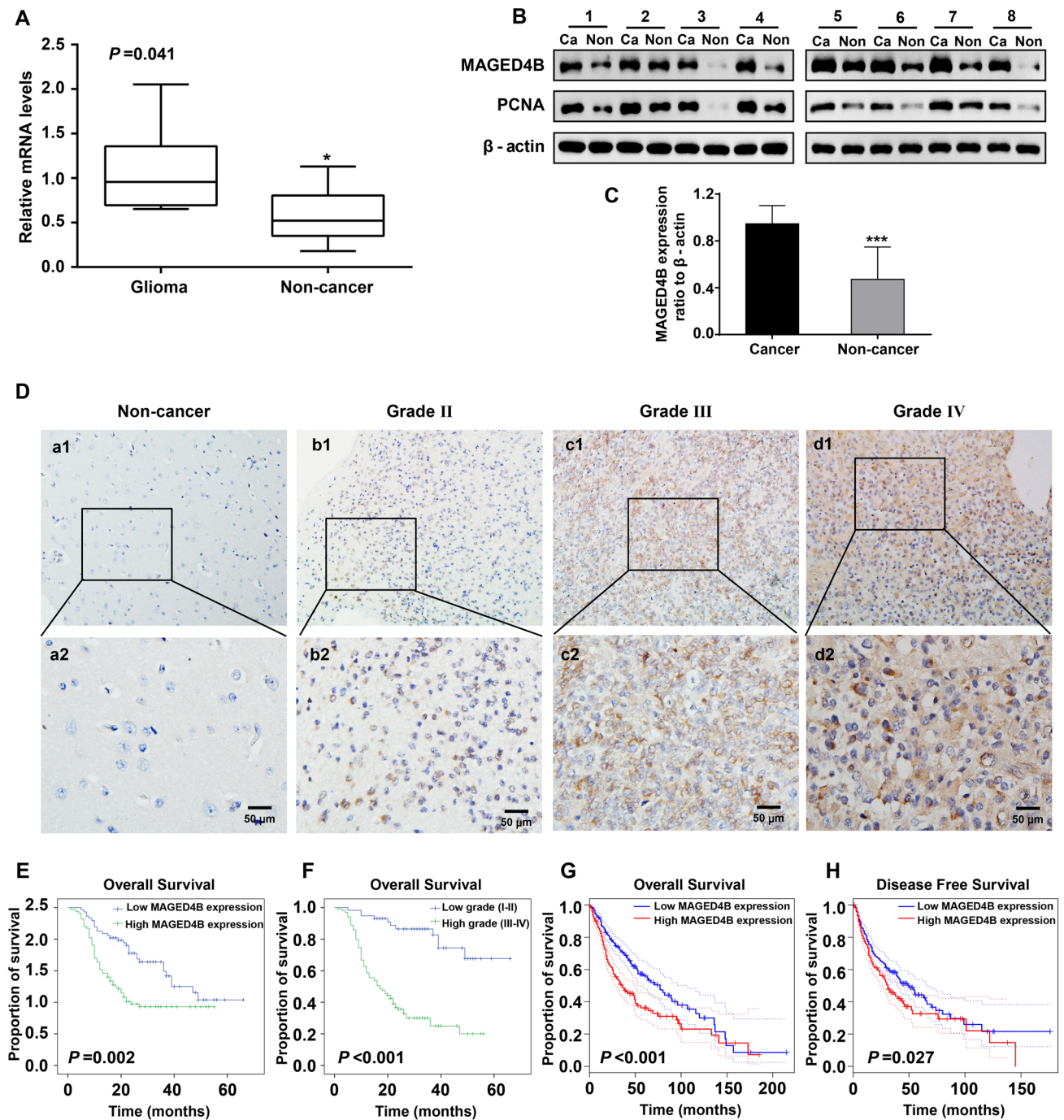


Fig. 1 MAGED4B expression in glioma and the association with survival. **A** Relative *MAGED4B* mRNA expression in glioma specimens and paired benign brain specimens ($n = 8$; $*P = 0.041$ vs glioma; t -test). **B** Western blots showing the protein levels of MAGED4B and PCNA in cancer tissue and matched non-cancer tissue of glioma patients. Ca, cancer tissue; Non, non-cancer tissue. **C** Quantitation of data as in **B** ($n = 8$; mean \pm SD; $***P < 0.001$ vs glioma; t -test). **D** Representative images of immunohistochemistry of

MAGED4B protein in glioma samples and adjacent tissue (scale bar, 50 μ m). **E** OS curves showing that survival of patients with a high MAGED4B level (green) is significantly lower than that of patients with a low level of MAGED4B (blue). **F** OS curves showing that survival is lower in patients with high-grade glioma (green) than that in patients with low-grade glioma (blue). **G**, **H** OS and DFS (disease-free survival) curves based on the GEPIA database through Kaplan-Meier analysis (as indicated). Kaplan-Meier analysis (**E–H**).

Table 1 Associations between MAGED4B expression and clinical attributes in glioma

Characteristic	<i>n</i>	MAGED4B expression, <i>n</i> (%)		Pearson χ^2	<i>P</i>
		Low expression	High expression		
Total	170	76 (46.50)	94 (53.50)		
Gender				0.380	0.538
Male	105	45 (42.86)	60 (57.14)		
Female	65	31 (47.69)	34 (52.31)		
Age (years)				7.338	0.007*
≤53	90	49 (54.44)	41 (45.56)		
>53	80	27 (33.75)	53 (66.25)		
Tumor diameter (cm)				4.153	0.042*
<5.0	77	41 (53.25)	36 (46.75)		
≥5.0	93	35 (37.63)	58 (62.37)		
Grade				6.966	0.008*
I–II	60	35 (58.33)	25 (41.67)		
III–IV	110	41 (37.27)	69 (62.73)		
P53				0.380	0.538
(–)	65	31 (47.69)	34 (52.31)		
(+)	105	45 (42.86)	60 (57.14)		
Ki67				6.707	0.010*
(–)	58	32 (55.17)	26 (44.83)		
(+)	84	28 (33.33)	56 (66.67)		
Unknown	28	16	22		
CD34				2.797	0.094
(–)	61	30 (49.18)	31 (50.82)		
(+)	77	27 (35.06)	50 (64.94)		
Unknown	32	19	13		

* *P* < 0.05.**Table 2** Univariate and multivariate analyses of prognostic factors of overall survival in glioma

	Univariate analysis		Multivariate analysis	
	HR (95% CI)	<i>P</i>	HR (95% CI)	<i>P</i>
Age (years) ≤53 vs >53	2.365 (1.502–3.725)	<0.001*	1.126 (0.666–1.903)	0.659
Gender Male vs female	0.782 (0.492–1.242)	0.298		
Grade I–II vs III–IV	6.110 (3.213–11.619)	<0.001*	5.047 (1.889–13.488)	0.001*
MAGED4B expression Low vs High	2.026 (1.287–3.188)	0.002*	2.084 (1.231–3.529)	0.006*
Tumor diameter (cm) <5.0 vs ≥5.0	0.910 (0.588–1.408)	0.670		
CD34 (–) vs (+)	1.558 (0.960–2.529)	0.073		
Ki67 (–) vs (+)	3.627 (2.035–6.465)	<0.001*	1.389 (0.701–2.753)	0.347
P53 (–) vs (+)	2.328 (1.403–2.864)	0.001*	1.141 (0.612–2.129)	0.677

* *P* < 0.05; HR: hazard ratio; 95% CI: 95% confidence interval.

Therefore, U87 cells were selected for stable transfection with sh-*MAGED4B*, and U251 cells were selected for HA-*MAGED4B* transfection. The transfection efficiency with the two shRNA lentiviral vectors was >80% (Fig. 2C). Subsequently, puromycin was used to select stable U87 cells infected with sh-NC or sh-*MAGED4B*. According to the results of Western blotting, the expression of endogenous *MAGED4B* was effectively inhibited by sh-*MAGED4B*, and sh-*MAGED4B*#2 exhibited a stronger inhibitory effect than sh-*MAGED4B*#1. Therefore, the U87 cells were stably transfected with sh-*MAGED4B*#2 and used for subsequent experiments (Fig. 2D). At the same time, rescue experiments were performed in U251 cells and U87 cells stably expressing sh-*MAGED4B* by co-transfecting them with HA-*MAGED4B* plasmid. We found that the protein level of *MAGED4B* was significantly increased in cells transfected with HA-*MAGED4B* (Fig. 2E).

MAGED4B Knockdown Attenuates Glioma Cell Proliferation in Vitro

The above data showed that *MAGED4B* expression in glioma tissue was positively correlated with tumor diameter and Ki-67 level (Table 1 and Fig. S2). Therefore, we hypothesized that *MAGED4B* may promote the proliferation of glioma. To test this hypothesis, EDU, CCK8, and clone formation assays were performed in U87 and U251 cells. We found that *MAGED4B* knockdown remarkably inhibited the viability of U87 cells, while *MAGED4B* overexpression increased the viability of U251 cells and U87 cells stably transfected with sh-*MAGED4B* (Fig. 3A). Moreover, EDU assays revealed that *MAGED4B* knockdown significantly

Fig. 2 Preparation and identification of glioma cell lines with *MAGED4B* overexpression or knockdown. **A** Western blots showing *MAGED4B* protein levels in U138, U251, and U87 cell lines. **B** Quantitation of data as in **A**. ($n = 2$, mean \pm SD). **C** Transfection efficiency of sh-*MAGED4B* in U87 cells. The plasmid is labeled with *GFP*, and green indicates successfully-transfected cells. **D** Western blots showing the efficacy of *MAGED4B* overexpression in U251 cells and U87 cells stably expressing sh-*MAGED4B*.

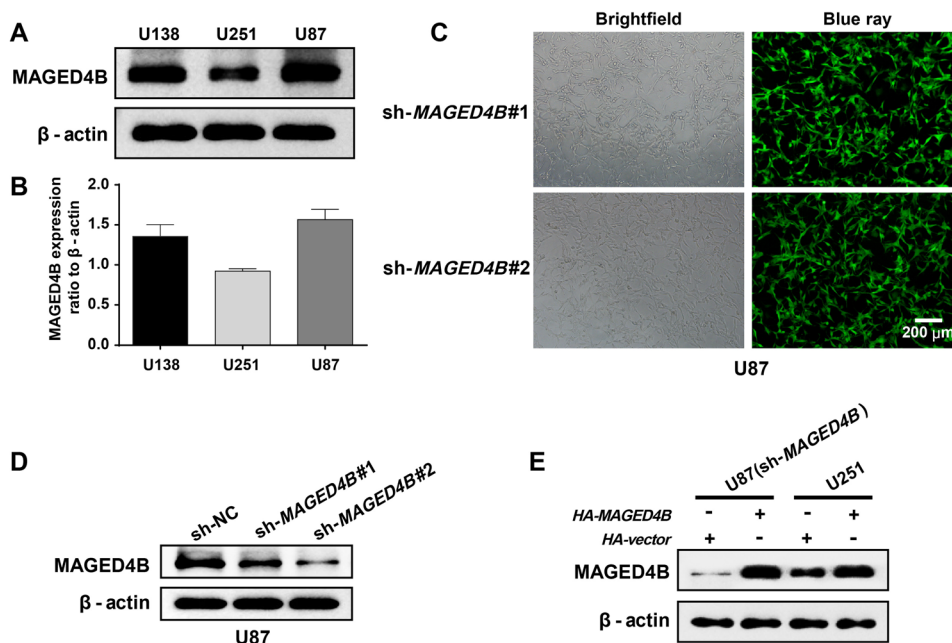
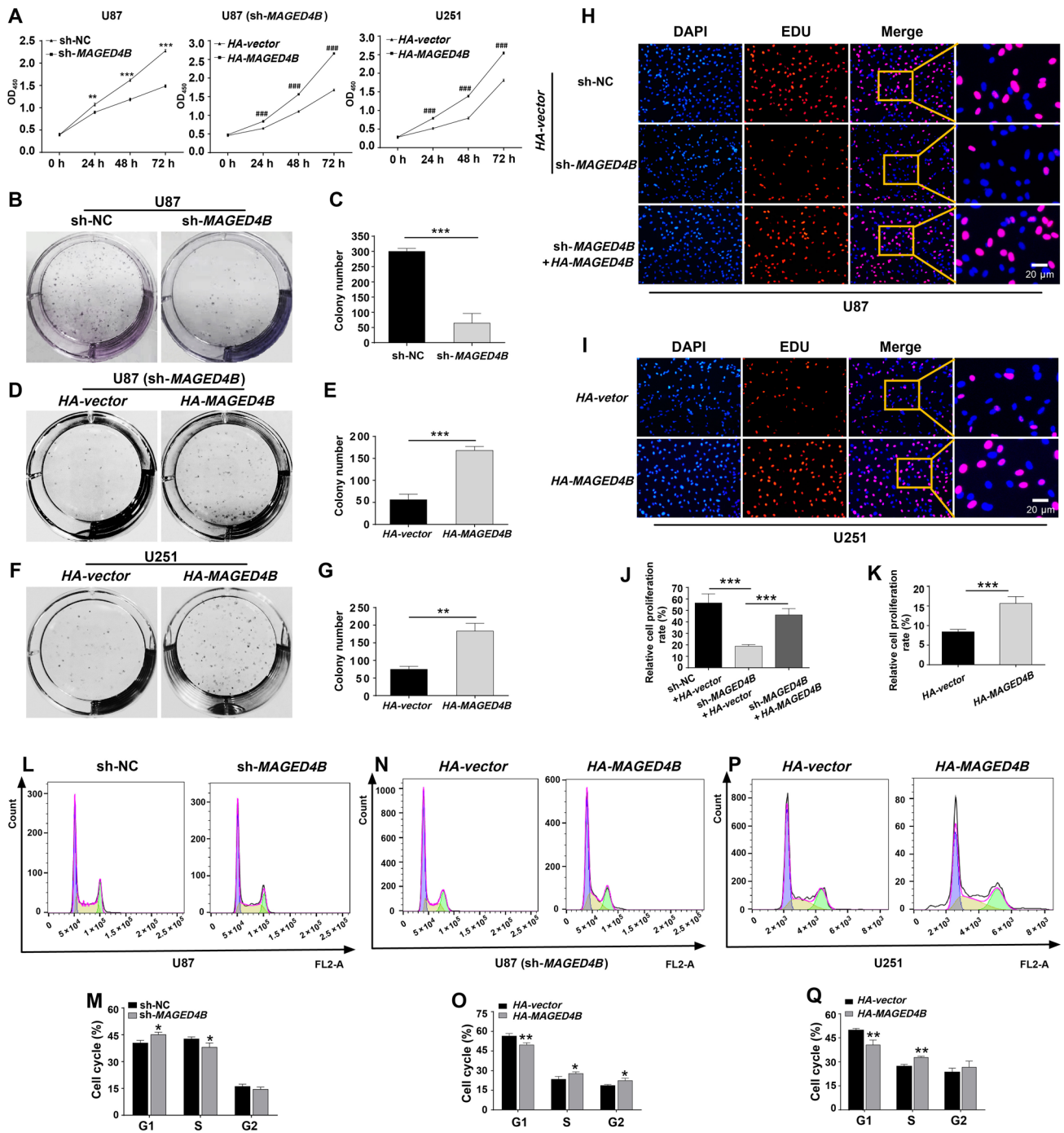


Fig. 3 *MAGED4B* promotes glioma cell proliferation. **A** Viability assessed by CCK8 assays at 0, 24, 48, and 72 h in U87 cells transfected with sh-*MAGED4B* (left), in U87 cells stably-expressing sh-*MAGED4B* transfected with HA-*MAGED4B* (middle), and U251 cells transfected with HA-*MAGED4B* (right) ($n = 3$; $***P < 0.01$, $***P < 0.001$ vs sh-NC; $###P < 0.001$ vs HA-vector; t -test). OD₄₅₀, optical density at 450 nm. **B–G** Numbers of cell colonies detected by colony formation assays in U87 (**B–E**) and U251 (**F, G**) cells. **B** U87 cells transfected with sh-NC or sh-*MAGED4B*. **C** Quantitation of data as in **B** ($n = 3$; $***P < 0.001$ vs sh-NC; t -test). **D** U87 cells stably expressing sh-*MAGED4B* transfected with HA-vector or HA-*MAGED4B*. **E** Quantitation of data as in **D** ($n = 3$; $***P < 0.001$ vs HA-vector; t -test). **F** U251 cells transfected with HA-vector or HA-*MAGED4B*. **G** Quantitation of data as in **F** ($n = 3$; $**P < 0.01$ vs HA-vector; t -test). **H** Viability of U87 cells assessed by EDU assay. U87 cells are transfected with sh-*MAGED4B* or sh-*MAGED4B* plus HA-*MAGED4B* (blue, nuclei stained with DAPI; red, EDU stained with Apollo in proliferating cells). **I** Viability of U251 cells assessed by EDU assays. U251 cells are transfected with HA-vector or HA-*MAGED4B* (blue, nuclei stained with DAPI; red, EDU stained with Apollo in proliferating cells). **J** Quantitation of data as in **H** ($n = 3$; $***P < 0.001$; one-way ANOVA followed by Tukey's test). **K** Quantitation of data as in **I** ($n = 3$; $***P < 0.001$ vs HA-vector; t -test). **L–Q** The cell cycle of U87 (**L–O**) and U251 (**P, Q**) cells as determined by flow cytometry. Purple, G1; yellow, S; green, G2. **L** U87 cells transfected with sh-NC or sh-*MAGED4B*. **M** Quantitation of data as in **L** ($n = 3$; $*P < 0.05$ vs sh-NC; t -test). **N** U87 cells stably expressing sh-*MAGED4B* and transfected with HA-vector or HA-*MAGED4B*. **O** Quantitation of data as in **N** ($n = 3$; $*P < 0.05$, $**P < 0.01$ vs HA-vector; t -test). **P** U251 cells transfected with HA-vector or HA-*MAGED4B*. **Q** Quantitation of data as in **P** ($n = 3$; $**P < 0.01$ vs HA-vector; t -test). All quantitative data are presented as the mean \pm SD.

suppressed proliferation in U87 cells, while *MAGED4B* overexpression enhanced proliferation in U251 cells and U87 cells stably transfected with sh-*MAGED4B* (Fig. 3H, I). Consistent with this, colony-formation experiments showed that *MAGED4B* knockdown inhibited the formation



of colonies, whereas *MAGED4B* overexpression enhanced the colony formation of U251 cells and U87 cells stably transfected with sh-*MAGED4B* (Fig. 3B–G). The above results suggest that *MAGED4B* promotes glioma cell proliferation. Next, flow cytometry was applied to investigate the effect of *MAGED4B* on the cell cycle in glioma cells. The results demonstrated that *MAGED4B* knockdown inhibited G1-S transition in U87 cells (Fig. 3L), while *MAGED4B* overexpression restored the effect caused by *MAGED4B*

knockdown in U87 and U251 cells (Fig. 3N, P). These data indicate that *MAGED4B* promotes cell proliferation by promoting cell viability and the G1-S transition.

MAGED4B Promotes Glioma Cell Invasion and Migration

Under the microscope, we observed that the length of the cell and cellular pseudopodia were shorter in U87

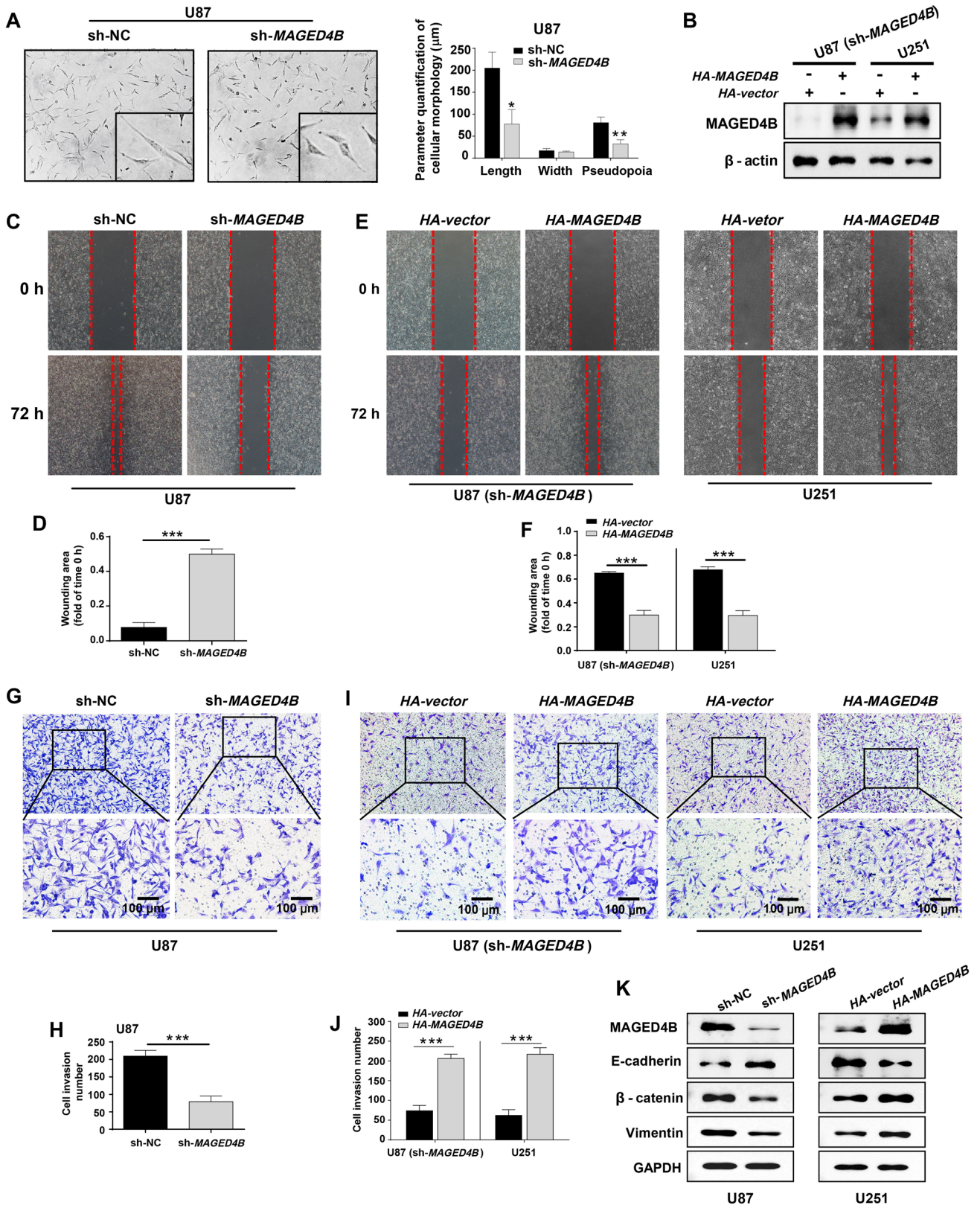


Fig. 4 MAGED4B promotes invasion and migration of glioma cells. **A** Left, bright field images showing the morphology of U87 cells stably transfected with sh-NC or sh-*MAGED4B*. Right, length and width of cells and length of pseudopodia measured using ImageJ software ($n = 3$; $*P < 0.05$, $**P < 0.01$ vs sh-NC; t -test). **B** Efficacy of *MAGED4B* overexpression in U251 cells and U87 cells stably transfected with sh-*MAGED4B*. β -actin is the loading control. **C–F** Migration of U87 and U251 cells assessed by wound-healing assays. Red dashed line, edge of cell scratch. **C** U87 cells transfected with sh-NC or sh-*MAGED4B*. **D** Quantitation of data as in **C** ($n = 3$; $***P < 0.001$ vs sh-NC; t -test). **E** U251 cells and U87 cells stably transfected with sh-*MAGED4B* and transfected with *HA*-vector or *HA-MAGED4B*. **F** Quantitation of data as in **E** ($n = 3$; $***P < 0.001$ vs *HA*-vector; t -test). **G–J** Cell invasion evaluated by transwell assays in U87 and U251 cells. **G** U87 cells transfected with sh-NC or sh-*MAGED4B*. **H** Quantitation of data as in **G** ($n = 3$; $***P < 0.001$ vs sh-NC; t -test). **I** U251 cells and U87 cells stably expressing sh-*MAGED4B* and transfected with *HA*-vector or *HA-MAGED4B*. **J** Quantitation of data as in **I** ($n = 3$; $***P < 0.001$ vs *HA*-vector; t -test). **K** *MAGED4B* knockdown up-regulates the level of E-cadherin, and down-regulates the levels of β -catenin and vimentin in U87 cells (cells are transfected with sh-NC or sh-*MAGED4B*). *MAGED4B* overexpression down-regulates the level of E-cadherin, and up-regulates the levels of β -catenin and vimentin in U251 cells (cells are transfected with *HA*-vector or *HA-MAGED4B*). All quantitative data are presented as the mean \pm SD.

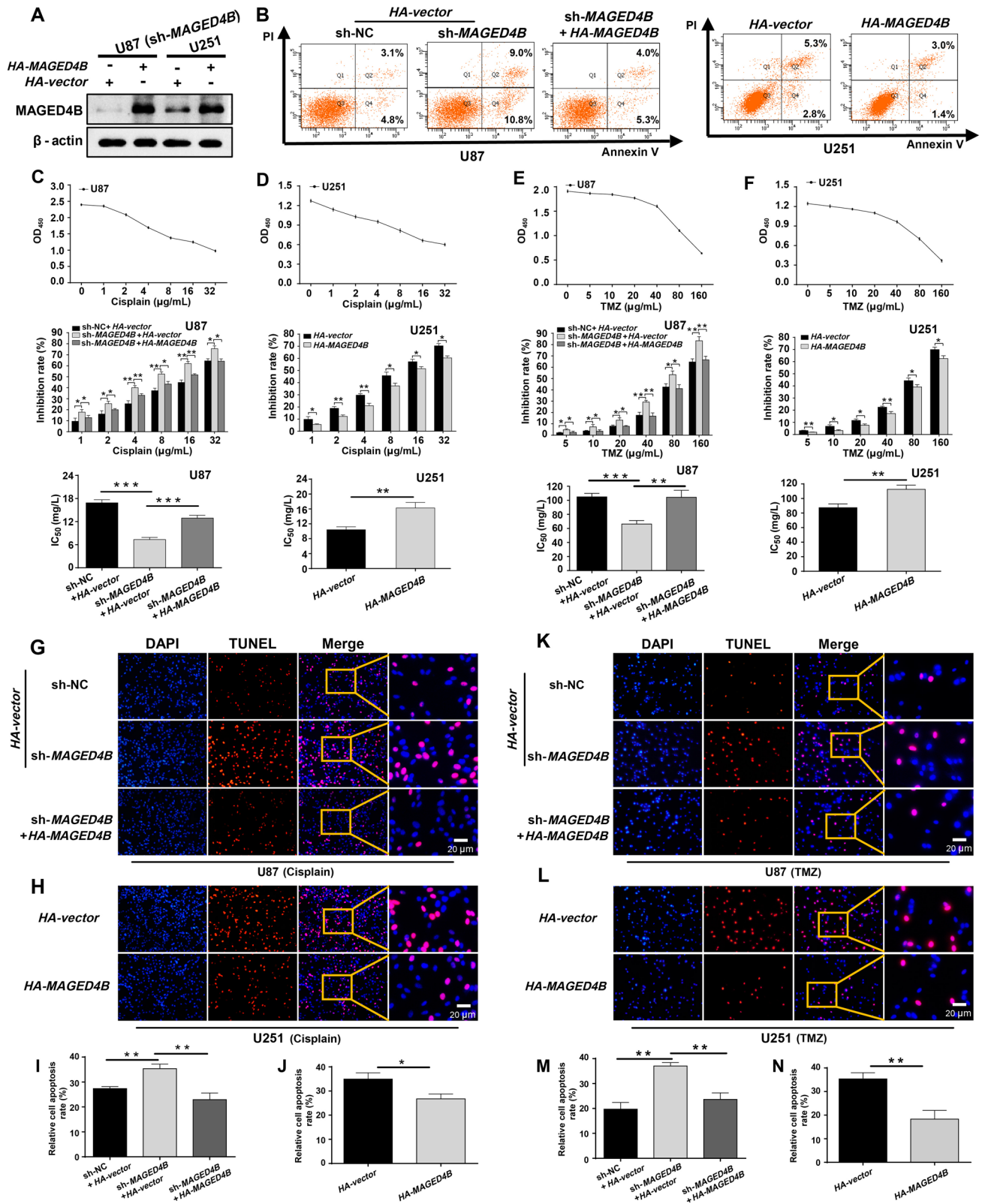
cells stably expressing sh-*MAGED4B* than in sh-NC cells (Fig. 4A), suggesting that *MAGED4B* promotes the migration of glioma cells. To confirm this, wound-healing and transwell tests were used to investigate the effect of *MAGED4B* on glioma migration and invasion. The transfection efficiency of *MAGED4B* overexpression with *HA-MAGED4B* was confirmed by Western blot analysis (Fig. 4B). The wound healing and transwell assays showed that *MAGED4B* knockdown significantly reduced the migratory and invasive ability in U87 cells, while *MAGED4B* overexpression rescued the inhibition of cell migration and invasion caused by *MAGED4B* knockdown. Similarly, in U251 cells, *MAGED4B* overexpression enhanced migration and invasion (Fig. 4C–J). These findings suggest that *MAGED4B* promotes invasion and migration in glioma. To explore whether *MAGED4B* affects glioma epithelial-mesenchymal transition (EMT), we assessed the protein levels of E-cadherin, β -catenin, and vimentin after knockdown or overexpression of *MAGED4B*. We found that *MAGED4B* knockdown up-regulated the protein level of E-cadherin and down-regulated the protein levels of β -catenin and vimentin. On the contrary, *MAGED4B* overexpression down-regulated the protein level of E-cadherin and up-regulated the protein levels of β -catenin and vimentin (Fig. 4K). These data indicate that *MAGED4B* promotes EMT in glioma.

MAGED4B Inhibits Apoptosis and the Sensitivity to Cisplatin and TMZ in Glioma

We have verified that *MAGED4B* promotes glioma cell proliferation. Many studies have shown that an increase in tumor cell proliferation can be attributed to the cell's ability to evade apoptosis [33, 34]. Accordingly, we investigated the effect of *MAGED4B* level on apoptosis. The expression efficacy of *MAGED4B* was confirmed by Western blot analysis (Fig. 5A). As expected, knockdown of endogenous *MAGED4B* induced a higher percentage of apoptotic cells than that in the controls, while *MAGED4B* overexpression inhibited apoptosis (Fig. 5B). Currently, TMZ is the most commonly-used chemotherapeutic agent for the clinical treatment of glioma [35]. Cisplatin, a chemotherapeutic drug widely applied for human solid malignancies, is currently used to treat malignant gliomas in combination with TMZ. To determine the effect of *MAGED4B* on the chemosensitivity of glioma cells to cisplatin and TMZ, the viability of glioma cells was determined by CCK8 assays. The results indicated that the viability was reduced by cisplatin and TMZ in a dose-dependent manner in U87 and U251 cells. *MAGED4B* overexpression decreased the sensitivity of glioma cells to cisplatin and TMZ. Furthermore, the IC_{50} of cisplatin and TMZ also reflected the same result. On the contrary, *MAGED4B* knockdown decreased the IC_{50} value and increased the sensitivity of glioma cells to cisplatin and TMZ (Fig. 5C–F). TUNEL assays were applied to further examine the effect of *MAGED4B* on the sensitivity of glioma cells to cisplatin and TMZ. After incubation with cisplatin (8 μ g/mL) for 24 h or TMZ (40 μ g/mL) for 48 h, the apoptosis of glioma cells was assessed. *MAGED4B* knockdown was found to facilitate cisplatin- and TMZ-induced apoptosis in U87 cells, while *MAGED4B* overexpression repressed cisplatin- and TMZ-induced apoptosis in U251 cells and U87 cells with stable *MAGED4B* knockdown (Fig. 5G–N). These results suggest that *MAGED4B* reduces the sensitivity of glioma cells to cisplatin and TMZ.

MAGED4B Promotes Glioma Growth in the Brains of Nude Rats

The above *in vitro* data suggest that *MAGED4B* promotes glioma cell proliferation and inhibits their apoptosis. In order to investigate the effects of *MAGED4B* on glioma growth *in vivo*, U87 cells stably transfected with sh-NC or sh-*MAGED4B* were injected into the brains of nude rats. The blank control was injected with PBS instead of U87 cells. As shown in Fig. 6A, the rat brains implanted with glioma cells were all larger than those with PBS, *MAGED4B* knockdown reduced the brain size compared with sh-NA controls. However, *MAGED4B* knockdown did not affect the body weight of nude rats implanted with the cells (Fig. 6B). To assess the



effect of MAGED4B on the size of glioma in rat brains, MRI images of tumors were obtained on day 16 after implantation. The results showed that the volume of gliomas in the

MAGED4B-knockdown group was smaller than that in the negative control group (Fig. 6C, D). Furthermore, immunohistochemical analysis showed that the staining intensity of

Fig. 5 MAGED4B inhibits apoptosis and sensitivity to cisplatin and TMZ in glioma. **A** Western blots verify the overexpression efficacy of MAGED4B in U251 and U87 cells with stably knocked down *MAGED4B*. **B** Flow cytometry showing apoptotic U87 and U251 cells. Left, U87 cells replenished with *HA-MAGED4B* after *MAGED4B* knockdown. Right, U251 cells transfected with *HA-vector* or *HA-MAGED4B*. **C, D** Upper, cell viability in CCK8 assays of U87 and U251 cells transfected as indicated after treatment with different concentrations of cisplatin. Middle, inhibition of U87 cells and U251 cells by cisplatin. Lower, IC_{50} of cisplatin in U87 and U251 cells. **E, F** Upper, viability assessed by CCK8 assays in U87 and U251 cells transfected as indicated after treatment with different concentrations of TMZ. Middle, inhibition of U87 cells and U251 cells by TMZ. Lower, IC_{50} of TMZ in U87 and U251 cells. $n = 3$; $*P < 0.05$, $**P < 0.01$, $***P < 0.001$; one-way ANOVA followed by Tukey's test (**C, E**), and t -test (**D, F**). **G–J** Apoptosis as detected by TUNEL assays in U251 and U87 cells 24 h after stimulation with 8 $\mu\text{g}/\text{mL}$ cisplatin. **G** U87 cells transfected with sh-*MAGED4B* or sh-*MAGED4B* plus *HA-MAGED4B*. **I** Quantitation of data as in **G** ($n = 3$; $**P < 0.01$; one-way ANOVA followed by Tukey's test). **H** U251 cells transfected with *HA-vector* or *HA-MAGED4B*. **J** Quantitation of data as in **H** ($n = 3$; $*P < 0.05$; t -test). **K–N** Apoptosis as detected by TUNEL assays in U251 and U87 cells 48 h after stimulation with 40 $\mu\text{g}/\text{mL}$ TMZ. **K** U87 cells transfected with sh-*MAGED4B* or sh-*MAGED4B* plus *HA-MAGED4B*. **M** Quantitation of data as in **K** ($n = 3$; $**P < 0.01$; one-way ANOVA followed by Tukey's test). **L** U251 cells transfected with *HA-vector* or *HA-MAGED4B*. **N** Quantitation of data as in **L** ($n = 3$; $**P < 0.01$; t -test). All quantitative data are presented as the mean \pm SD.

MAGED4B in the control group was significantly stronger than that in the *MAGED4B*-knockdown group (Fig. 6E), suggesting that MAGED4B was effectively knocked down in the implanted U87 cells. The above results demonstrated that MAGED4B promotes glioma growth *in vivo*.

MAGED4B Promotes TRIM27 Ubiquitination and Inhibits the TNF- α -related Apoptotic Pathway in Glioma Cells

Previous reports have shown that the MAGE proteins can interact with RING finger proteins and regulate tumor progression. TRIM27 is known to be an E3 ubiquitin ligase with the RING finger domain. In the present study, the interaction of MAGED4B and TRIM27 was predicted by the STRING database (<https://string-db.org/>) (Fig. 7A). Subsequently, the interaction between TRIM27 and MAGED4B was confirmed by Co-IP assays (Fig. 7B). In addition, the co-localization of MAGED4B and TRIM27 was detected by immunofluorescence staining, which revealed remarkable co-localization in the cytoplasm of U87 cells (Fig. 7C). These data indicate that MAGED4B interacts with TRIM27 in gliomas. Meanwhile, we found that *MAGED4B* overexpression down-regulated the TRIM27 protein level, and *MAGED4B* knockdown up-regulated it (Fig. 7D, E). To assess the effect of MAGED4B on TRIM27 protein stability, we assessed the protein level of TRIM27 in glioma cells after cycloheximide treatment.

The results showed that *MAGED4B* overexpression significantly reduced the half-life of TRIM27 (Fig. 7F, G). More importantly, MAGED4B-mediated TRIM27 down-regulation was inhibited by MG132 (Fig. 7H), suggesting that the proteasome is involved in MAGED4B-mediated TRIM27 degradation. Consistent with this, we found that *MAGED4B* overexpression increased the level of ubiquitinated TRIM27 by using the Co-IP assay with an anti-TRIM27 antibody (Fig. 7I).

It has been reported that TRIM27 promotes apoptosis through the TNF- α -related apoptotic pathway *via* regulating the USP7/RIP1 interaction [25, 36]. In the present study, we also found that *MAGED4B* overexpression downregulated the protein levels of RIP1, caspase-8, caspase-3, and cleaved caspase-3 (Fig. 7D). On the contrary, *MAGED4B* knockdown up-regulated the levels of the above proteins (Fig. 7E). These results suggest that MAGED4B may inactivate the TNF- α -related apoptotic pathway by promoting TRIM27 degradation (Fig. 8).

Discussion

In this study, we found that the MAGED4B level in glioma tissue was increased, which was closely associated with a poor clinical outcome. Subsequently, we demonstrated the promoting role of MAGED4B in cell proliferation, invasion and migration, tumor growth, and drug resistance. In addition, we demonstrated the interaction of MAGED4B with TRIM27 and found that MAGED4B enhanced TRIM27 ubiquitination and degradation, which inhibited TNF- α -related apoptosis in glioma. These findings indicate that MAGED4B may be used as a biomarker for glioma diagnosis and a potential target for glioma therapy.

MAGEs were initially identified as tumor-specific antigens due to their characteristic expression patterns; since then, MAGE type I proteins have been widely studied as attractive indicators for tumor immunotherapy [9–11]. MAGED4B is a type II MAGE protein. An increasing number of studies have shown that the expression of MAGED4B is significantly restricted in normal tissues [8, 37, 38], and a high MAGED4B level has been documented in several types of cancer, such as breast cancer [13], oral squamous cell carcinoma [14], glioma [16], and non-small cell lung cancer [12]. However, the studies on MAGED4B in glioma are limited and contradictory. He *et al.* reported the expression of MAGED4B in samples from 41 cases of glioma, and assessed the relationship between MAGED4B expression and the clinicopathological characteristics of patients. The results showed that MAGED4B expression was not significantly correlated with tumor grade [18]. Another study analyzed the relationship between MAGED4B expression and

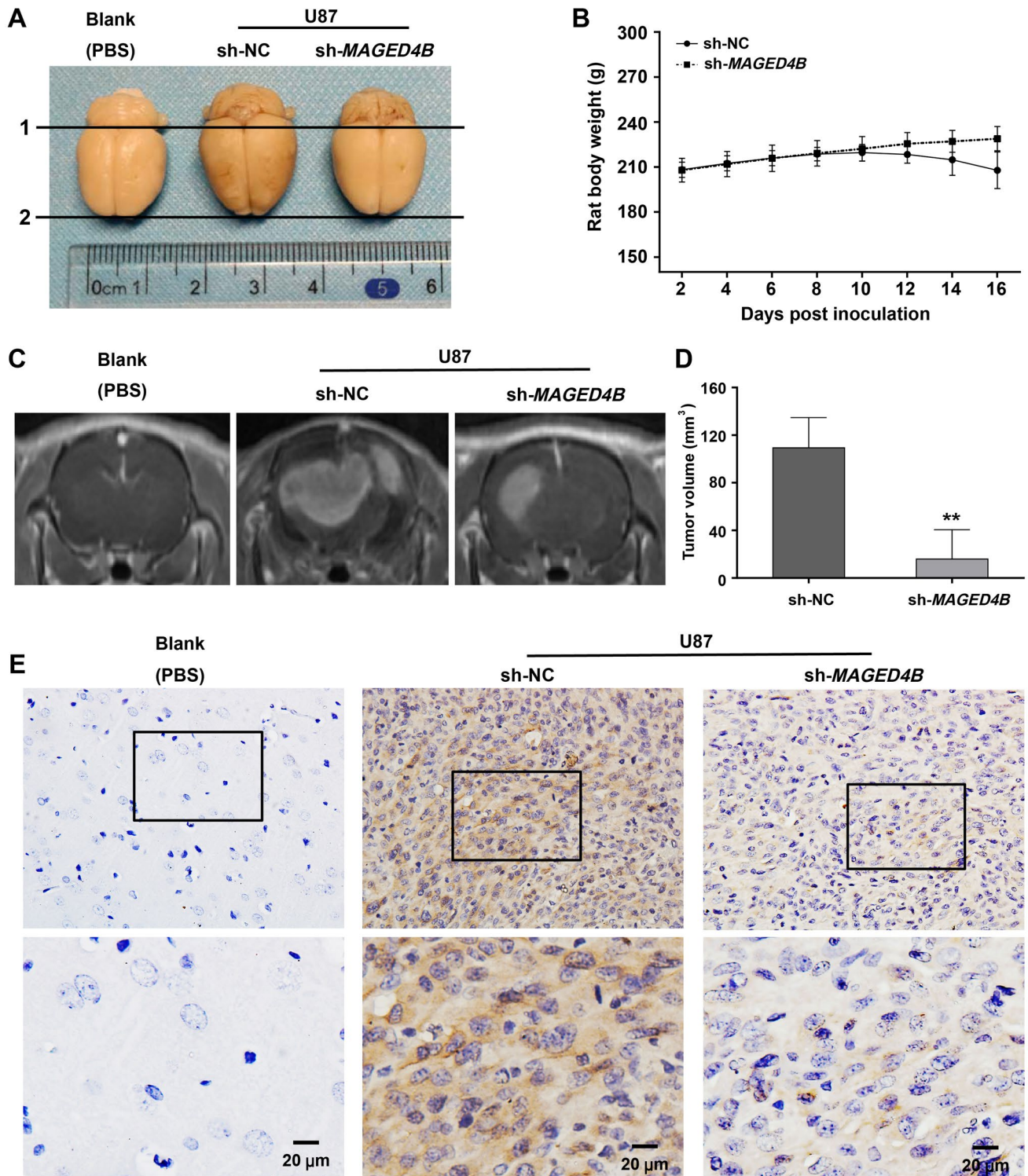


Fig. 6 MAGED4B promotes glioma growth *in vivo*. **A** Brains from nude rats implanted with U87 cells stably transfected with sh-NC or sh-MAGED4B (1, upper edge of rat brains; 2, lower edge of rat brains). **B** Time-course curves of body weight measured every 2 days in the negative controls and *MAGED4B*-knockdown rats ($n = 5$; mean \pm SD). **C** Contrast-enhanced T1-weighted images of tumors on day

16 after implantation of U87 cells stably transfected with sh-NC or sh-MAGED4B. **D** Tumor volume measured from MRI images ($n = 5$; mean \pm SD; ** $P < 0.01$ vs sh-NC; t -test). **E** Representative immunohistochemistry images of MAGED4B expression in nude rat brain samples implanted with U87 cells stably expressing sh-NC or sh-MAGED4B.

clinicopathological parameters in samples from 124 cases of glioma, and the results showed that MAGED4B expression was significantly correlated with the tumor grade and p53 expression [16]. These studies are contradictory and lack functional studies of MAGED4B in glioma. Therefore, the effect of MAGED4B in glioma needs to be further investigated. In this study, we applied IHC assays to assess MAGED4B expression in 170 cancer samples and 30 non-cancer tissues from glioma patients and found that MAGED4B was significantly elevated in the cancer samples. We also found that MAGED4B expression was positively correlated with glioma grade, tumor diameter, Ki-67 level, and patient age, consistent with the Cancer Genome Atlas (TCGA) and TIMER data. In the TCGA database, a high MAGED4B level was associated with advanced tumor grade. In the TIMER database, the up-regulated MAGED4B level was related to Ki-67 overexpression. In addition, our results demonstrated that overexpression of MAGED4B was correlated with a poor prognosis of glioma patients. Similarly, Germano *et al.* found that higher MAGED4B expression in breast cancer is associated with lower survival rates [13]. The above results preliminarily indicate that MAGED4B has a universal value in evaluating tumor prognosis.

Our data demonstrated that overexpression of *MAGED4B* promoted glioma cell growth both *in vivo* and *in vitro*. The evidence from the Ki67 index in glioma samples and proliferation experiments *in vitro* indicated that this is attributed to the increased proliferation of glioma cells with high MAGED4B levels. This viewpoint is in accordance with previous studies on breast cancer and oral squamous cell carcinoma, which suggest that high proliferative activity is associated with the elevated expression of MAGED4B [13, 14]. The tendency of cancer cells to metastasize and invade is recognized as a hallmark of cancer [39]. In the present study, we found that overexpression of *MAGED4B* enhanced the invasion and migration capacity of glioma cells. Previous reports have shown that MAGED4B promotes the invasion and metastasis of breast cancer cells, but in oral cancer, MAGED4B only promotes metastasis. It is suggested that the differences may be related to the specificity of cell types and/or experimental methods. Indeed, both MAGED1 and MAGED4B are MAGE type II proteins and have the same homology domain. Surprisingly, overexpression of *MAGED1* has been reported to inhibit cell cycle progression and reduce cell invasion and migration [40–42]. We hypothesize that these different results might be due to the different amino terminals of MAGED4B and MAGED1 [43, 44]. One of the hallmarks of cancer is the ability of cancer cells to elude apoptosis [33, 34]. Currently, TMZ is commonly used as the first-line agent for glioma treatment [35]. Cisplatin has been used as an adjuvant with TMZ in glioma treatment [45]. Here, we found that knockdown of *MAGED4B* promoted the apoptosis of glioma cells, and overexpression

of *MAGED4B* reduced cisplatin- and TMZ-induced apoptosis, indicating that high MAGED4B expression could help glioma cells evade apoptosis, thus promoting cell proliferation. This finding is in accordance with previous research findings where MAGEA was documented to inhibit Bax expression in myeloma cells, thus inhibiting apoptosis [46]. Moreover, it has been reported that the MAGEA, MAGEB, and MAGEC proteins can bind to KRAB-associated protein 1 (KAP1) to inhibit P53-dependent apoptosis [47].

An increasing body of evidence suggests that the homology domain of MAGE proteins can bind to and regulate E3 RING finger proteins [19, 21, 44]. The TRIM proteins constitute a large E3 ubiquitin ligase family and are involved in MAGE-RING complexes, which are involved in a variety of cellular processes, including proliferation, cell cycle regulation, and apoptosis [21, 48]. Previous studies have reported that both type I and type II MAGEs bind to specific TRIM E3 RING ligases (including TRIM27, TRIM28, and TRIM31). It has been reported that MAGEA1-TRIM31 plays a role in the cellular immune response [48], while the MAGEL2-TRIM27-USP7 complex plays an important role in neurodevelopmental disorders by promoting retromer recycling [49]. MAGEA2, MAGEA3, MAGEA6, and MAGEC2 bind to TRIM28 and inhibit p53-mediated apoptosis [19–21]. However, the relationship between MAGED4B and TRIM E3 RING ligase remains elusive. In order to explore the possible mechanism underlying MAGED4B-mediated tumor promotion, we evaluated the protein-protein interactions of MAGED4B and TRIM proteins using the STRING database [50], and interaction was found between MAGED4B and TRIM27. Furthermore, a Co-IP assay was used to confirm the interaction between MAGED4B and TRIM27. TRIM27 belongs to the family of TRIM proteins, and plays a dual role in regulating apoptosis [23, 24]. It has been reported that TRIM27 activates the c-Jun N-terminal kinase (JNK)/p38 signaling pathway, thereby promoting apoptosis and inhibiting cell survival [51]. In liver cancer cells, TRIM27 reportedly forms a complex with USP7, which positively regulates TNF- α -induced apoptosis [25], while TRIM27 overexpression in ovarian cancer and renal cancer inhibits apoptosis [52, 53]. In HeLa cells, TRIM27 interacts with HDAC and inhibits apoptosis [26].

It has been reported that TRIM27 ubiquitinates USP7, while the latter de-ubiquitinates RIP1-(Ub)_n in TNF complex I and up-regulates the expression of RIP1, which promotes TNF complex II formation and up-regulates the expression of downstream apoptotic proteins and then leads to apoptosis [25, 36]. Our study revealed an interaction between MAGED4B and TRIM27: MAGED4B enhanced the ubiquitination and degradation of TRIM27. Subsequently, the molecules downstream of TRIM27/USP7, including RIP1, caspase-8, caspase-3, and cleaved caspase-3, were correspondingly decreased by MAGED4B. RIP1, caspase-8,

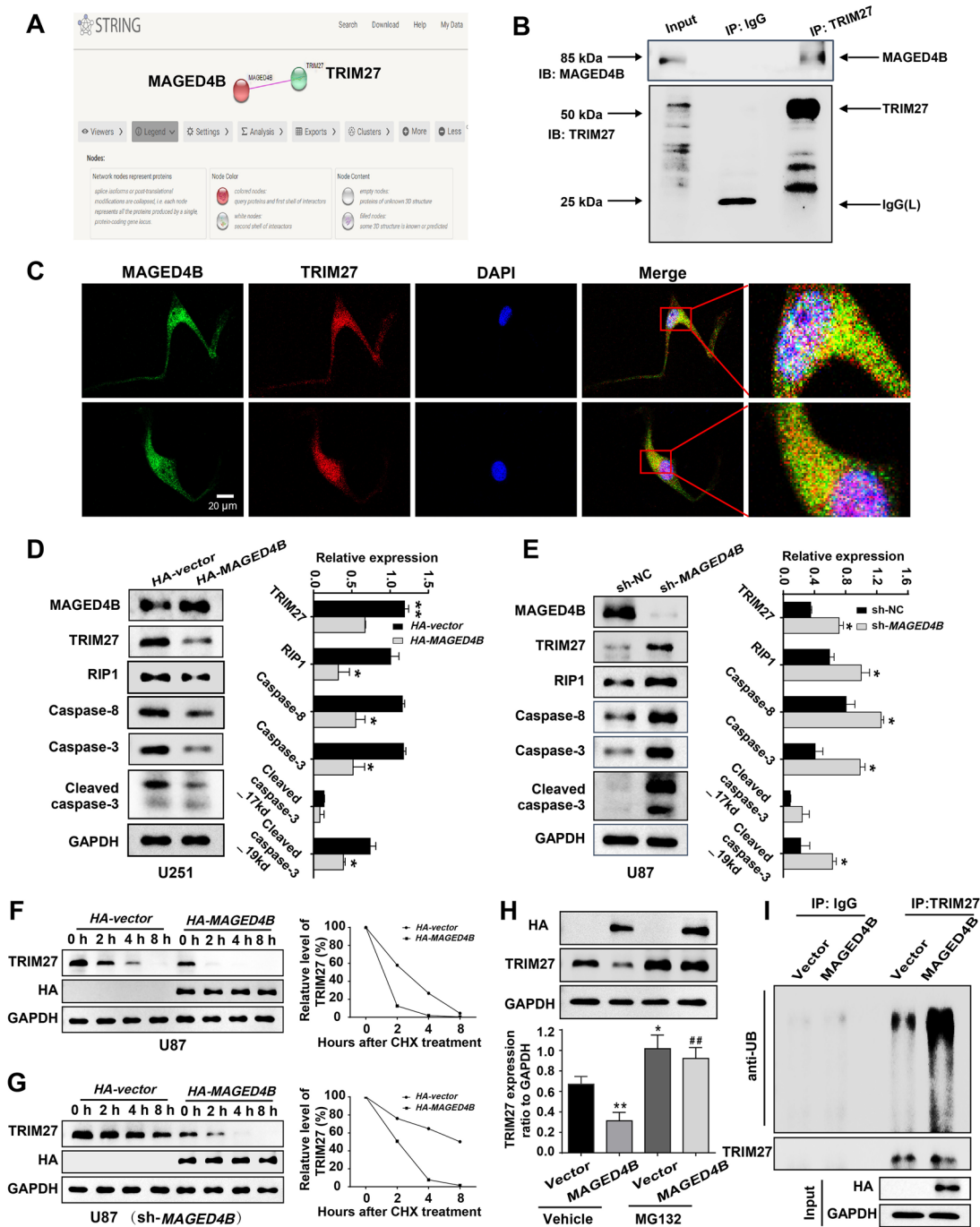


Fig. 7 MAGED4B interacts with TRIM27 and targets its downstream genes involved in the TNF- α -related apoptotic pathway. **A** Prediction of interaction between MAGED4B and TRIM27 from the STRING database. **B** Interaction between MAGED4B and TRIM27 detected by Co-IP assay in U87 cells using an anti-TRIM27 antibody. **C** Immunofluorescence staining showing co-localization of MAGED4B (green) and TRIM27 (red) in U87 cells [nuclei are stained with DAPI (blue)]. **D** MAGED4B overexpression down-regulates the levels of TRIM27 and TNF- α -related apoptotic pathway markers (RIP1, caspase-8, caspase-3, and cleaved caspase-3) in U251 cells. The cells are transfected with HA-vector or HA-MAGED4B. ($n = 3$; $*P < 0.05$, $**P < 0.01$ vs HA-vector; t -test). **E** MAGED4B knockdown up-regulates the levels of TRIM27 and TNF- α -related apoptotic pathway markers (RIP1, caspase-8, caspase-3, and cleaved caspase-3) in U87 cells. The

cells are transfected with sh-NC or sh-MAGED4B. ($n = 3$; $*P < 0.05$ vs sh-NC; t -test). **F**, **G** Effect of treatment of cycloheximide (CHX; 20 μ g/mL) on the levels of TRIM27 protein in U87 cells after transfection with HA-vector or HA-MAGED4B. **F** MAGED4B overexpression reduces the half-life of TRIM27 in U87 cells. **G** MAGED4B overexpression reduces the half-life of TRIM27 in U87 cells stably transfected with sh-MAGED4B. **H** The proteasome inhibitor MG132 inhibits the reduction of TRIM27 induced by MAGED4B overexpression in U87 cells [cells were treated with MG132 (20 mmol/L) for 8 h] ($n = 3$; $*P < 0.05$, $**P < 0.01$ vs vector; $##P < 0.01$ vs MAGED4B without MG132; one-way ANOVA followed by Tukey's test). **I** MAGED4B overexpression increases TRIM27 ubiquitination in U87 cells in the presence of MG132 (20 mmol/L). All quantitative data are presented as the mean \pm SD.

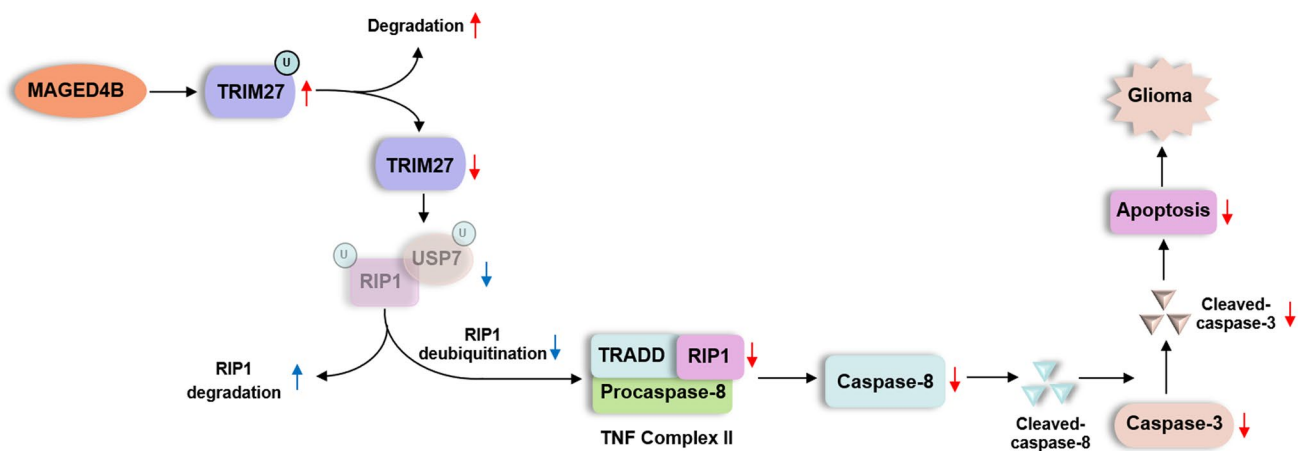


Fig. 8 Schematic of the effect of MAGED4B on glioma progression by down-regulating TRIM27. It has been reported that TRIM27, an E3 ubiquitin ligase, ubiquitinates USP7 for USP7-induced RIP1 deubiquitination (blue arrows), which up-regulates TNF complex II-dependent apoptosis. Here, we found that MAGED4B down-regulates the TRIM27 protein level and promotes the development of glioma

by promoting TRIM27 ubiquitination, which inactivates the TNF complex II-dependent apoptosis (red arrows). MAGED4B, MAGE family member D4B; TRIM27, tripartite motif-containing 27; USP7, ubiquitin-specific protease 7; RIP1, receptor-interacting serine/threonine-protein kinase 1; TRADD, TNFRSF1A-associated via death domain; TNF, tumor necrosis factor.

caspase-3, and cleaved caspase-3 are apoptosis-related markers, and the decrease in the levels of these proteins reflects the low rate of apoptosis. Therefore, these findings suggest that TRIM27 plays a role in promoting apoptosis *via* the TNF- α -related apoptotic pathway in glioma. Previous research has reported that MAGEs function as regulators of E3 RING finger ubiquitin ligases. Studies have shown that MAGEs can bind to TRIM28 and UbcH2 at the same time, and then enhance the ubiquitination of both TRIM28 and its substrates [21, 44]. Similarly, the current study implies that MAGED4B suppresses the apoptosis of glioma cells by promoting the ubiquitination of TRIM27, subsequently inactivating the TNF- α -related apoptotic pathway in glioma cells. Interestingly, it has been reported that TRIM27 interacts with HDAC1 and inhibits apoptosis in MGMT-positive glioblastoma cells [27]. In the present study, U87 and U251 were used as MGMT-negative cell lines. In MGMT-positive cell lines, IFN- α markedly increased TMZ anti-tumor activity, but not in MGMT-negative cell lines [54]. Sunitinib significantly reduces the angiogenesis activity of MGMT-positive cells but not that of MGMT-negative cells [55]. We hypothesize that the roles of TRIM27 are dependent on the specificity of cell types and context. This is in accordance with previous findings showing that TRIM8 promotes the self-renewal of glioblastoma stem-like cells (N08-30 and N13-213) through activating signal transducer and activator of transcription 3 (STAT3) signaling. However, TRIM8 inhibits mitosis in U87 cells (low-stemness) by interacting with KIFC1 and KIF11 [56, 57]. In future studies, we will further investigate these issues.

In summary, we revealed that MAGED4B is up-regulated in glioma compared to non-cancerous brain tissue. Moreover, high expression of MAGED4B promotes the proliferation, invasion, and migration, and suppresses apoptosis of glioma cells, and this is related to its capability to ubiquitinate TRIM27 and inhibit the activity of the TNF- α -related apoptotic pathway. Our study uncovers the potential molecular mechanism of MAGED4B in glioma. The data provide a basis for future clinical studies investigating the use of MAGED4B as a biomarker to predict and treat glioma patients.

Acknowledgments This work was supported by the National Natural Science Foundation of China (81801679 and 81571308).

Conflict of interest The authors have declared that no competing interest exists.

References

1. Lin Z, Yang R, Li K, Yi G, Li Z, Guo J. Establishment of age group classification for risk stratification in glioma patients. *BMC Neurol* 2020, 20: 310.
2. Weller M, Wick W, Aldape K, Brada M, Berger M, Pfister SM, *et al.* Glioma. *Nat Rev Dis Primers* 2015, 1: 15017.
3. Wang PG, Li YT, Pan Y, Gao ZZ, Guan XW, Jia L, *et al.* Lower expression of Bax predicts poor clinical outcome in patients with glioma after curative resection and radiotherapy/chemotherapy. *J Neurooncol* 2019, 141: 71–81.
4. Zhang C, Zhang Z, Li F, Shen Z, Qiao Y, Li L, *et al.* Large-scale analysis reveals the specific clinical and immune features of B7–H3 in glioma. *Oncoimmunology* 2018, 7: e1461304.
5. Mihelson N, McGavern DB. Viral control of glioblastoma. *Viruses* 2021, 13: 1264.

6. van der Bruggen P, Traversari C, Chomez P, Lurquin C, de Plaen E, van den Eynde B, *et al.* A gene encoding an antigen recognized by cytolytic T lymphocytes on a human melanoma. *Science* 1991, 254: 1643–1647.
7. Chi DD, Merchant RE, Rand R, Conrad AJ, Garrison D, Turner R, *et al.* Molecular detection of tumor-associated antigens shared by human cutaneous melanomas and gliomas. *Am J Pathol* 1997, 150: 2143–2152.
8. Barker PA, Salehi A. The MAGE proteins: Emerging roles in cell cycle progression, apoptosis, and neurogenetic disease. *J Neurosci Res* 2002, 67: 705–712.
9. Wu Y, Sang M, Liu F, Zhang J, Li W, Li Z, *et al.* Epigenetic modulation combined with PD-1/PD-L1 blockade enhances immunotherapy based on MAGE-A11 antigen-specific CD8+T cells against esophageal carcinoma. *Carcinogenesis* 2020, 41: 894–903.
10. Zajac P, Schultz-Thater E, Tornillo L, Sadowski C, Trella E, Mengus C, *et al.* MAGE-A antigens and cancer immunotherapy. *Front Med (Lausanne)* 2017, 4: 18.
11. Schooten E, di Maggio A, van Bergen En Henegouwen PMP, Kijanka MM. MAGE-A antigens as targets for cancer immunotherapy. *Cancer Treat Rev* 2018, 67: 54–62.
12. Ito S, Kawano Y, Katakura H, Takenaka K, Adachi M, Sasaki M, *et al.* Expression of MAGE-D4, a novel MAGE family antigen, is correlated with tumor-cell proliferation of non-small cell lung cancer. *Lung Cancer* 2006, 51: 79–88.
13. Germano S, Kennedy S, Rani S, Gleeson G, Clynes M, Doolan P, *et al.* MAGE-D4B is a novel marker of poor prognosis and potential therapeutic target involved in breast cancer tumorigenesis. *Int J Cancer* 2012, 130: 1991–2002.
14. Chong CE, Lim KP, Gan CP, Marsh CA, Zain RB, Abraham MT, *et al.* Over-expression of MAGED4B increases cell migration and growth in oral squamous cell carcinoma and is associated with poor disease outcome. *Cancer Lett* 2012, 321: 18–26.
15. Krämer BF, Schoor O, Krüger T, Reichle C, Müller M, Weinschenk T, *et al.* MAGED4-expression in renal cell carcinoma and identification of an HLA-A*25-restricted MHC class I ligand from solid tumor tissue. *Cancer Biol Ther* 2005, 4: 943–948.
16. Yan J, Wen J, Wei ZD, Li XS, Li P, Xiao SW. Prognostic and clinicopathological value of melanoma-associated antigen D4 in patients with glioma. *Oncol Lett* 2018, 15: 4151–4160.
17. Takami H, Kanda M, Oya H, Hibino S, Sugimoto H, Suenaga M, *et al.* Evaluation of MAGE-D4 expression in hepatocellular carcinoma in Japanese patients. *J Surg Oncol* 2013, 108: 557–562.
18. He SJ, Gu YY, Yu L, Luo B, Fan R, Lin WZ, *et al.* High expression and frequently humoral immune response of melanoma-associated antigen D4 in glioma. *Int J Clin Exp Pathol* 2014, 7: 2350–2360.
19. Doyle JM, Gao J, Wang J, Yang M, Potts PR. MAGE-RING protein complexes comprise a family of E3 ubiquitin ligases. *Mol Cell* 2010, 39: 963–974.
20. Jin X, Pan Y, Wang L, Zhang L, Ravichandran R, Potts PR, *et al.* MAGE-TRIM28 complex promotes the Warburg effect and hepatocellular carcinoma progression by targeting FBP1 for degradation. *Oncogenesis* 2017, 6: e312.
21. Feng Y, Gao J, Yang M. When MAGE meets RING: Insights into biological functions of MAGE proteins. *Protein Cell* 2011, 2: 7–12.
22. Micale L, Chaignat E, Fusco C, Reymond A, Merla G. The tripartite motif: Structure and function. *Adv Exp Med Biol* 2012, 770: 11–25.
23. Hatakeyama S. TRIM family proteins: Roles in autophagy, immunity, and carcinogenesis. *Trends Biochem Sci* 2017, 42: 297–311.
24. Hatakeyama S. TRIM proteins and cancer. *Nat Rev Cancer* 2011, 11: 792–804.
25. Zaman MMU, Nomura T, Takagi T, Okamura T, Jin W, Shinagawa T, *et al.* Ubiquitination-deubiquitination by the TRIM27-USP7 complex regulates tumor necrosis factor alpha-induced apoptosis. *Mol Cell Biol* 2013, 33: 4971–4984.
26. Kato T, Shimono Y, Hasegawa M, Jijiwa M, Enomoto A, Asai N, *et al.* Characterization of the HDAC1 complex that regulates the sensitivity of cancer cells to oxidative stress. *Cancer Res* 2009, 69: 3597–3604.
27. Ranjit M, Hirano M, Aoki K, Okuno Y, Ohka F, Yamamichi A, *et al.* Aberrant active cis-regulatory elements associated with down-regulation of RET finger protein overcome chemoresistance in glioblastoma. *Cell Rep* 2019, 26: 2274–2281.e5.
28. Liu J, Wu Z, Han D, Wei C, Liang Y, Jiang T, *et al.* Mesencephalic astrocyte-derived neurotrophic factor inhibits liver cancer through small ubiquitin-related modifier (SUMO)ylation-related suppression of NF- κ B/snail signaling pathway and epithelial-mesenchymal transition. *Hepatology* 2020, 71: 1262–1278.
29. Chen P, Liu C, Li P, Wang Q, Gao X, Wu H, *et al.* High RhCG expression predicts poor survival and promotes migration and proliferation of gastric cancer *via* keeping intracellular alkaline. *Exp Cell Res* 2020, 386: 111740.
30. Camp RL, Dolled-Filhart M, Rimm DL. X-tile: a new bio-informatics tool for biomarker assessment and outcome-based cut-point optimization. *Clin Cancer Res* 2004, 10: 7252–7259.
31. Apostolou A, Shen Y, Liang Y, Luo J, Fang S. Armet, a UPR-upregulated protein, inhibits cell proliferation and ER stress-induced cell death. *Exp Cell Res* 2008, 314: 2454–2467.
32. Tang Z, Li C, Kang B, Gao G, Li C, Zhang Z. GEPIA: a web server for cancer and normal gene expression profiling and interactive analyses. *Nucleic Acids Res* 2017, 45: W98–W102.
33. Neophytou CM, Trougakos IP, Erin N, Papageorgis P. Apoptosis deregulation and the development of cancer multi-drug resistance. *Cancers (Basel)* 2021, 13: 4363.
34. Modi S, Kir D, Banerjee S, Saluja A. Control of apoptosis in treatment and biology of pancreatic cancer. *J Cell Biochem* 2016, 117: 279–288.
35. Zhao P, Wang Y, Kang X, Wu A, Yin W, Tang Y, *et al.* Dual-targeting biomimetic delivery for anti-glioma activity *via* remodeling the tumor microenvironment and directing macrophage-mediated immunotherapy. *Chem Sci* 2018, 9: 2674–2689.
36. Nie D, Zhang D, Dai J, Zhang M, Zhao X, Xu W, *et al.* Nicotine induced murine spermatozoa apoptosis *via* up-regulation of deubiquitinated RIP1 by Trim27 promoter hypomethylation. *Biol Reprod* 2016, 94: 31.
37. Zhang QM, He SJ, Shen N, Luo B, Fan R, Fu J, *et al.* Overexpression of MAGE-D4 in colorectal cancer is a potentially prognostic biomarker and immunotherapy target. *Int J Clin Exp Pathol* 2014, 7: 3918–3927.
38. Chomez P, de Backer O, Bertrand M, de Plaen E, Boon T, Lucas S. An overview of the MAGE gene family with the identification of all human members of the family. *Cancer Res* 2001, 61: 5544–5551.
39. Lah TT, Novak M, Breznik B. Brain malignancies: Glioblastoma and brain metastases. *Semin Cancer Biol* 2020, 60: 262–273.
40. Tian XX, Rai D, Li J, Zou C, Bai Y, Wazer D, *et al.* BRCA2 suppresses cell proliferation *via* stabilizing MAGE-D1. *Cancer Res* 2005, 65: 4747–4753.
41. Du Q, Zhang Y, Tian XX, Li Y, Fang WG. MAGE-D1 inhibits proliferation, migration and invasion of human breast cancer cells. *Oncol Rep* 2009, 22: 659–665.
42. Salehi AH, Roux PP, Kubu CJ, Zeindler C, Bhakar A, Tannis LL, *et al.* NRAGE, a novel MAGE protein, interacts with the p75 neurotrophin receptor and facilitates nerve growth factor-dependent apoptosis. *Neuron* 2000, 27: 279–288.

43. Sasaki A, Hinck L, Watanabe K. RumMAGE-D the members: Structure and function of a new adaptor family of MAGE-D proteins. *J Recept Signal Transduct Res* 2005, 25: 181–198.
44. Lee AK, Potts PR. A comprehensive guide to the MAGE family of ubiquitin ligases. *J Mol Biol* 2017, 429: 1114–1142.
45. Wang Y, Kong X, Guo Y, Wang R, Ma W. Continuous dose-intense temozolomide and cisplatin in recurrent glioblastoma patients. *Medicine* 2017, 96: e6261.
46. Nardiello T, Jungbluth AA, Mei A, Diliberto M, Huang X, Dabrowski A, *et al.* MAGE-A inhibits apoptosis in proliferating myeloma cells through repression of Bax and maintenance of survivin. *Clin Cancer Res* 2011, 17: 4309–4319.
47. Yang B, O'Herrin SM, Wu J, Reagan-Shaw S, Ma Y, Bhat KM, *et al.* MAGE-A, mMage-b, and MAGE-C proteins form complexes with KAP1 and suppress p53-dependent apoptosis in MAGE-positive cell lines. *Cancer Res* 2007, 67: 9954–9962.
48. Kozakova L, Vondrova L, Stejskal K, Charalabous P, Kolesar P, Lehmann AR, *et al.* The melanoma-associated antigen 1 (MAGEA1) protein stimulates the E3 ubiquitin-ligase activity of TRIM31 within a TRIM31-MAGEA1-NSE4 complex. *Cell Cycle* 2015, 14: 920–930.
49. Tacer KF, Potts PR. Cellular and disease functions of the Prader-Willi Syndrome gene *MAGEL2*. *Biochem J* 2017, 474: 2177–2190.
50. Szklarczyk D, Franceschini A, Wyder S, Forslund K, Heller D, Huerta-Cepas J, *et al.* STRING v10: Protein-protein interaction networks, integrated over the tree of life. *Nucleic Acids Res* 2015, 43: D447–D452.
51. Wang J, Teng JL, Zhao D, Ge P, Li B, Woo PC, *et al.* The ubiquitin ligase TRIM27 functions as a host restriction factor antagonized by Mycobacterium tuberculosis PtpA during mycobacterial infection. *Sci Rep* 2016, 6: 34827.
52. Xiao C, Zhang W, Hua M, Chen H, Yang B, Wang Y, *et al.* TRIM27 interacts with I κ b α to promote the growth of human renal cancer cells through regulating the NF- κ B pathway. *BMC Cancer* 2021, 21: 841.
53. Jiang J, Xie C, Liu Y, Shi Q, Chen Y. Up-regulation of miR-383-5p suppresses proliferation and enhances chemosensitivity in ovarian cancer cells by targeting TRIM27. *Biomed Pharmacother* 2019, 109: 595–601.
54. Ni XR, Guo CC, Yu YJ, Yu ZH, Cai HP, Wu WC, *et al.* Combination of levetiracetam and IFN- α increased temozolomide efficacy in MGMT-positive glioma. *Cancer Chemother Pharmacol* 2020, 86: 773–782.
55. Chahal M, Xu Y, Lesniak D, Graham K, Famulski K, Christensen JG, *et al.* MGMT modulates glioblastoma angiogenesis and response to the tyrosine kinase inhibitor sunitinib. *Neurooncology* 2010, 12: 822–833.
56. Zhang C, Mukherjee S, Tucker-Burden C, Ross JL, Chau MJ, Kong J, *et al.* TRIM8 regulates stemness in glioblastoma through PIAS3-STAT3. *Mol Oncol* 2017, 11: 280–294.
57. Venuto S, Monteonofrio L, Cozzolino F, Monti M, Appolloni I, Mazza T, *et al.* TRIM8 interacts with KIF11 and KIFC1 and controls bipolar spindle formation and chromosomal stability. *Cancer Lett* 2020, 473: 98–106.

Springer Nature or its licensor holds exclusive rights to this article under a publishing agreement with the author(s) or other rightsholder(s); author self-archiving of the accepted manuscript version of this article is solely governed by the terms of such publishing agreement and applicable law.